A simple approach for probabilistic internal stability analysis and design of reinforced soil walls

Richard J. Bathurst & Nezam Bozorgzadeh
GeoEngineering Centre at Queen's-RMC, Royal Military College of Canada, Kingston, Ontario, Canada

ABSTRACT
This paper explains probabilistic analysis and design for simple internal stability limit states for mechanically stabilized earth (MSE) walls using the example of steel grid reinforced soil walls. The general approach uses a closed-form solution for reliability index which is easily implemented in a spreadsheet and thus eliminates the need for Monte Carlo simulation. A novel feature of the formulation is that it includes uncertainty in the choice of nominal values [which is consistent with the notion of level of understanding that appears in the Canadian Highway Bridge Design Code] and the underlying accuracy of the load and resistance models that appear in each limit state equation using bias statistics. The paper demonstrates how bias statistics for tensile load and pullout model accuracy can be gathered from load measurements recorded from instrumented walls and found in laboratory pullout box test databases. The concepts are general and can be applied to any soil-structure interaction problem which can be expressed by a simple linear limit state performance function and for which bias statistics are available.

RÉSUMÉ
Cet article explique l'analyse et la conception probabiliste pour des états limites de stabilité interne simples des murs en terre stabilisée mécaniquement, en utilisant l'exemple des murs en sols renforcés par une grille en acier. L'approche générale utilise une solution analytique pour l'indice de fiabilité qui est facilement implémentée dans un tableur et élimine ainsi le besoin de simulation de Monte Carlo. Une nouvelle caractéristique de la formulation est qu'elle inclut une incertitude dans le choix des valeurs nominales [ce qui est compatible avec la notion de niveau de compréhension qui figure dans le Code de conception des ponts-routes du Canada] et la précision sous-jacente des modèles de charge et de résistance qui apparaissent dans chaque équation d'état limite utilisant des statistiques de biais. Le document montre comment les statistiques de biais pour la charge de traction et la précision du modèle d'arrachement peuvent être collectées à partir de mesures de charge enregistrées sur des murs instrumentés et celles trouvées dans des bases de données d'essais d'arrachement en laboratoire. Les concepts sont généraux et peuvent être appliqués à tout problème d'interaction sol-structure qui peut être exprimé par une simple fonction de performance à état limite linéaire et pour lequel des statistiques de biais sont disponibles.

1 INTRODUCTION

The design and analysis of geotechnical structures is moving towards reliability-based design (RBD). RBD provides an alternative approach to allowable stress design (ASD) and load and resistance factor design (LRFD) which is found in North American LRFD codes (e.g. AASHTO 2017; CHBDC 2019). The former is familiar to geotechnical engineers as the global factor of safety approach. The disadvantage of the ASD approach is that two limit state solutions with the same factor of safety are unlikely to have the same margin of safety in probabilistic terms. In the current US and Canadian LRFD codes the foundation sections are not true reliability-based codes because the load and resistance factors have been computed based on fitting to factor of safety past practice. If a limit state function is satisfied at the time of design using these codes, the engineer is assured that the design is safe; however, how safe in a reliability (or probability of failure) context is unknown.

The most recent edition of the Canadian Highway Bridge Design Code CHBDC (2019) has for the first time a section on LRFD for mechanically stabilized earth (MSE) walls. This has been one motivation to investigate true RBD for internal stability limit states for these structures.

2 PRELIMINARIES

The general problem can be referenced to Figure 1 which shows the principal components of a steel grid MSE wall of height H and width L. The two ultimate limit states of interest are tensile rupture of the steel reinforcement and

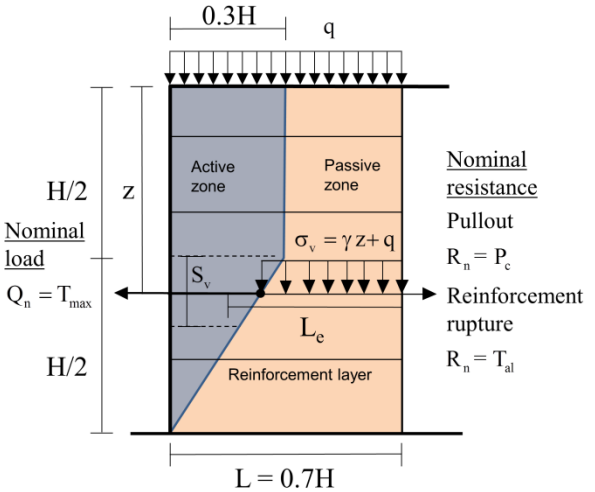

Figure 1. Problem geometry and reinforcement rupture and pullout limit states for steel grid walls.

pullout of the reinforcement from the passive zone. Here, $Q_n = T_{max}$ is the nominal maximum tensile load in the reinforcement layer under operational conditions and R_n is the nominal ultimate pullout resistance ($R_n = P_c$), or the nominal allowable tensile strength of the reinforcement layer ($R_n = T_{al}$). Both limit states are expressed as:

$$g = \frac{R_n \lambda_R}{Q_n \lambda_Q} - 1 \qquad [1]$$

Parameters λ_R and λ_Q are bias values that transform nominal values to measured (observed) values. The ratio of R_n/Q_n can be recognized as the familiar nominal factor of safety which is the starting point for any design regardless that the design approach is ASD, LRFD or RBD. If the models to compute measured (observed) values were perfect then bias values would be 1. Of course, this is an unrealistic expectation in geotechnical engineering practice and the limit state models for internal stability of MSE walls are no exception. Fortunately, bias values for the load and resistance models used by designers of MSE walls have been collected by the author and co-workers and published in a number of publications. These bias values are used in the present study to demonstrate the general approach.

All of the parameters in Equation 1 have uncertainty. For example, the nominal load and nominal pullout capacity are a function of soil unit weight which has some uncertainty. The yield strength of the steel also has some variability albeit rather small. The bias values that appear in Equation 1 were originally computed by taking the ratio of an observed value (i.e. measured load or resistance) to the matching predicted nominal value using the model equations that appear in AASHTO (2017) and CHBDC (2019). Each population of bias values is characterized by a statistical mean and coefficient of variation (COV). The uncertainty in the calculation of nominal values of load and resistance from all sources is assigned a single value of COV = 0.1, 0.2 and 0.3 corresponding to high, typical and low "level of understanding" as adopted in Canadian foundation engineering practice (CHBDC 2019; Fenton et al. 2017). If the quality and quantity of the material properties are typical for similar projects, the designer is experienced with the technology and the wall project is straightforward, then COV = 0.2 matching typical conditions. If project conditions and knowledge fall below or above typical conditions, then values of COV = 0.3 and 0.1 are recommended, respectively. Clearly, levels of understanding are subjective and the design engineer in concert with other stakeholders (e.g. the owner) must decide which level of understanding applies to project conditions. Guidance on this self-evaluation process for the case of reinforcement pullout can be found in the paper by Bathurst et al. (2017). The exception to the nominal COV values reproduced above is the use of COV = 0 for the reinforcement strength which is taken as deterministic at time of design and thus COV = 0.

Finally, in order to focus on the basics, the example used in this paper assumes that there is negligible or no corrosion of the steel members over the life of the wall. This is a reasonable assumption for many walls since steel members are galvanized in practice to minimize loss of steel due to corrosion and specifications for the backfill call for soils that are electro-chemically non-aggressive.

3 LOAD AND RESISTANCE MODELS

The load model in this paper is the Coherent Gravity Method that appears in the US AASHTO (2017) and Canadian (CHBDC 2019) LRFD codes. The maximum load T_{max} in a reinforcement layer located at depth z is:

$$T_{max} = K_r S_v \sigma_v = K_r S_v (\gamma z + q) \qquad [2]$$

Here, parameter S_v = contributory area (spacing) of the layer, K_r = (empirical) coefficient of earth pressure which is a function of the peak soil friction angle ϕ and depth of reinforcement layer z. Parameter $\sigma_v = \gamma z + q$ is the vertical pressure acting at the elevation of the reinforcement layer, γ = soil unit weight and q = uniform surcharge pressure.

The tensile strength limit state is expressed as:

$$T_{al} = F_y A \qquad [3]$$

Here, F_y is the yield strength of the steel and A is the sum of the cross-section areas of the steel longitudinal members per m running length of the wall face. It should be noted that in North American practice the nominal yield strength of the steel is used for the tensile strength limit state even though this is an ultimate limit state (AASHTO 2017; CHBDC 2019). In North American codes the minimum specified yield strength is F_y = 450 MPa.

The pullout capacity model used in this study is the current recommended model in US (AASHTO 2017) and Canadian (CHBDC 2019) specifications for steel grids and can be expressed as:

$$P_c = n_b b t \sigma_v N_q R_c \qquad [4]$$

where P_c = pullout capacity (e.g. kN/m), n_b = number of transverse bars, b is the transverse bar length = width of the steel grid element (e.g. units of m), t = transverse bar thickness (m), N_q is a dimensionless bearing capacity factor, and R_c = coverage ratio computed as the ratio of b/S_h where S_h = the centre-to-centre spacing of each steel grid repeating unit. Typical repeating units are constructed with 2 to 6 longitudinal bars.

4 CALCULATION OF RELIABILITY INDEX

Reliability index (β) is used in this paper to quantify level of safety. Larger β values correspond to lower probabilities of failure. In fact, probability of failure (P_f) and reliability index can be equated using the approximation $P_f = 1 - \Phi(\beta)$ where Φ is the standard normal cumulative distribution function (NORMSDIST function in Excel).

The calculation of β can be carried out using Monte Carlo simulation or approximations such as the first order

reliability method. However, this approach is not familiar to many design engineers and is often viewed as tedious. In addition, the method may be computationally expensive if target reliability index values are very large. A more convenient and informative approach is to use a closed-form solution developed by Bathurst and Javankhoshdel (2017) and appears here as Equation 5.

$$\beta = \frac{\ln\left[\left(\frac{\mu_{\lambda R}\mu_{Rn}}{\mu_{\lambda Q}\mu_{Qn}}\right)\sqrt{\frac{(1+COV_{Qn}^2)(1+COV_{\lambda Q}^2)}{(1+COV_{Rn}^2)(1+COV_{\lambda R}^2)}}\right]}{\sqrt{\ln\left[\frac{(1+COV_{Qn}^2)(1+COV_{\lambda Q}^2)(1+COV_{Rn}^2)(1+COV_{\lambda R}^2)(1+\rho_R COV_{Rn} COV_{\lambda R})^2 (1+\rho_Q COV_{Qn} COV_{\lambda Q})^2}{(1+\rho_n COV_{Rn} COV_{Qn})^2}\right]}} \quad [5]$$

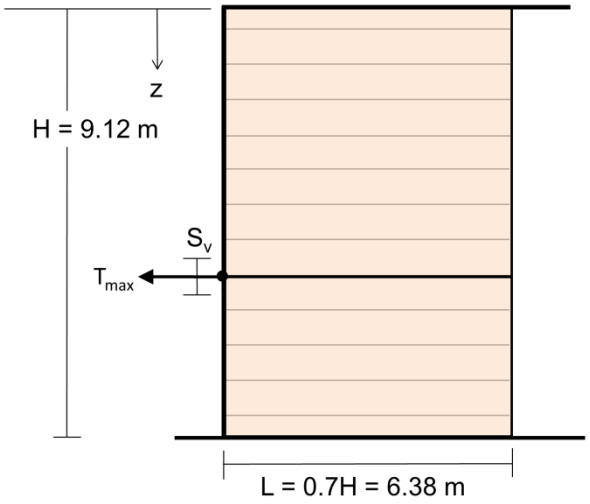

Figure 2. Problem geometry and reinforcement layout for example wall (after Allen and Bathurst 2018).

Table 1. Reinforcement (after Allen and Bathurst 2018).

Layer number	Depth z (m)	Unit width b (mm)	Number of longitudinal bars per unit	Bar diameter (mm)	Transverse bar spacing (mm)
12	0.38	600	4	6	305
11	1.14	800	5	6.4	305
10	1.90	1000	6	7.6	305
9	2.66	1000	6	7.6	305
8	3.42	1000	6	8.8	305
7	4.18	1000	6	8.8	305
6	4.94	1000	6	8.8	305
5	5.70	1000	6	8.8	610
4	6.46	1000	6	8.8	610
3	7.22	1000	6	9.5	610
2	7.98	1000	6	9.9	610
1	8.74	1000	6	10.7	610

Here, μ_{Rn} and COV_{Rn}, μ_{Qn} and COV_{Qn}, $\mu_{\lambda R}$ and $COV_{\lambda R}$, and $\mu_{\lambda Q}$ and $COV_{\lambda Q}$ are mean and COV values for R_n, Q_n, λ_R and λ_Q, respectively. Parameters ρ_R and ρ_Q are bias dependencies which are the Pearson correlation coefficients between R_n and λ_R and between Q_n and λ_Q, respectively. When ρ_R and ρ_Q are non-zero, the corresponding resistance bias and load bias values vary with the magnitude of the nominal values (R_n and Q_n). Parameter ρ_n is the correlation coefficient between R_n and Q_n and is non-zero when equations for R_n and Q_n share one or more input parameters that are random variables. Hereafter, ρ_n is referred to as nominal correlation for brevity.

5 EXAMPLE WALL

Figure 2 shows the example wall that is used here to carry out reliability analysis for the two limit states of interest introduced earlier. The steel grid reinforcement arrangement is summarized in Table 1. The wall is based on an example field wall reported by Allen and Bathurst (2018) with some modifications to the bar diameters to produce a design which is optimized with respect to current LRFD design recommendations in AASHTO (2017). The peak soil friction angle for this wall is $\phi = 34°$ and the soil unit weight is $\gamma = 21.8$ kN/m^3.

6 MODEL BIAS DATA

6.1 Load bias data

Figure 3a show the cumulative distribution function (CDF) plot for load bias values. Each load bias value (λ_Q) was computed by taking the ratio of a measured (observed) load in an instrumented steel grid layer to the matching predicted (nominal) value using the Coherent Gravity Method. A total of 81 measurements from 18 instrumented wall sections were available for this purpose (Allen and Bathurst 2018). The walls were constructed with frictional soils. The data largely plot as a straight line using a horizontal logarithmic scale, at least visually. This means that the data can be practically assumed to be lognormally distributed. The approximation to the CDF plot can be computed using the calculated mean of all bias values ($\mu_{\lambda Q} = 1.28$) and the calculated COV of all bias values ($COV_{\lambda Q} = 0.45$). The mean bias value shows that the measured load values are 28% higher than the predicted (nominal) values *on average*. Furthermore,

Table 2. Bias statistics for load and resistance models.

Model	Number of data points	Bias		
		Mean	COV	Dependency [(d)]
Coherent Gravity Method [(a)]	81	1.28	0.45	-0.34
Tensile strength [(b)], F_y	NA	1.10	0.07	0
Pullout [(c)]	129	1.33	0.44	-0.44

(a) Allen and Bathurst (2018); (b) Typical statistics from literature; (c) Miyata et al. (2018) using fit to all pullout bias data; (d) correlation (ρ) between bias and nominal value

there is significant spread in model accuracy (i.e., $COV_{\lambda Q}$ = 0.45). Closer scrutiny of the fit to all bias data shows that the approximation does poorly at the lower tail. However, this is not a practical concern because it is the distribution of load bias values at the upper tail that strongly influences reliability analysis outcomes. These values represent data where the measured (observed) loads were greater than the predicted values and hence these data contribute to greater probability of failure while the data at the lower tail do not.

Load bias values are plotted against predicted (nominal) values in Figure 3b. The data show that the accuracy of the model varies with magnitude of the predicted load value using the Coherent Gravity Method. For example, the under-prediction of the measured observed load values is greater at low nominal values than at high values. This is an undesirable feature of any load model but can be accommodated explicitly using the closed-form solution introduced earlier (Equation 5) with $\rho_{\lambda Q}$ = -0.34.

6.2 Pullout bias data

Figure 4a shows bias data computed from 129 steel grid pullout box tests with the steel grid specimens embedded in frictional soils (Miyata et al. 2018). The bias values (λ_R) were computed in the same manner as described for the load bias values. Each measured (observed) pullout capacity value from a pullout test was divided by the predicted value using Equation 4. In this plot the fitted approximation can be argued to do poorly at the upper tail of the distribution. However, this is not a practical concern because measured pullout values that are greater than predicted values do not contribute to probability of failure. The fit to lower tail is likely accurate enough for the purposes of reliability analyses. However, the fit to the lower tail could be locally improved by selecting a different combination of mean and COV of pullout bias. This is shown in the plot. Reliability analysis outcomes presented later in this paper are based on the fit to all data since the general approach is the same regardless of which set of bias values are used.

Pullout bias values are plotted against predicted (nominal) values of pullout capacity in Figure 4b to quantify the dependency of pullout model accuracy on the magnitude of computed pullout values. The data trend is similar to that for the load bias data discussed earlier but the correlation is stronger ($\rho_{\lambda Q}$ = -0.44).

Table 2 summarizes the bias data used in this paper to carry out reliability analyses for the two limit states of interest.

7 RESULTS

7.1 Tensile strength limit state

Figure 5 shows the results of reliability calculations for each reinforcement layer using the bias statistics for load (T_{max}) and tensile strength (T_{al}). Reliability index (β) values have been transformed to probability of failure (P_f) using the standard normal cumulative distribution function mentioned earlier. The calculations carried out in this paper assume that no corrosion of the steel members has taken place at the end of design life (e.g. 75 years). Stated alternatively, the protective galvanization layer has not been consumed at any location on the steel bars.

The variability in the value of tensile strength is captured by the bias values of μ_λ= 1.10 and $COV_{\lambda R}$ = 0.07 shown in Table 2. Potential correlations between nominal load (Q_n) and nominal resistance (R_n), and between nominal resistance and bias resistance are zero. Hence in Equation 5, $\rho_n = \rho_Q = 0$. This is because the strength of the steel (Equation 3) is independent of the value of the parameters that appear in the equation for maximum tensile load in the reinforcement layer (Equation 2). Regardless, because COV_{Rn} = 0, the bottommost parenthetical term in the denominator of Equation 5 disappears.

In the calculations for the plots in Figure 5, uncertainty in the value of the nominal load is assumed as zero (COV_{Qn} = 0) which is an idealized situation, and also as COV_{Qn} = 0.1, 0.2 and 0.3 following the three levels of understanding discussed earlier. For $COV_{Qn} > 0$, the probability of failure is less than for the case for COV_{Qn} = 0 for cases with non-zero probabilities of failure. Furthermore, for the same non-zero values of COV_{Qn}, the probability of failure does not change consistently with decreasing magnitude of COV_{Qn}. These observations appear counter intuitive but are the result of the interplay between parameters in Equation 5. The same result occurs using Monte Carlo simulation. Nevertheless, these observations are not of practical importance because for all cases the maximum probability of failure is less than P_f = 1%. A probability of failure of 1% (or reliability index value β = 2.33) is accepted as a target value in current LRFD calibration practice for the internal stability limit states for MSE walls (Allen et al. 2005). This is because these systems are highly strength redundant. If one reinforcement layer fails, the other layers of reinforcement can compensate. The sharp changes in the trend of the data at different depths for each plot in this figure are due to changes in the number of longitudinal bars per layer, width of the bar elements (units) and bar diameters (see Table 1).

7.2 Pullout limit state

Figure 6 shows probability of pullout failure for the same layers in the example wall. It should be noted that for this limit state, nominal load (Q_n) and resistance (R_n) values

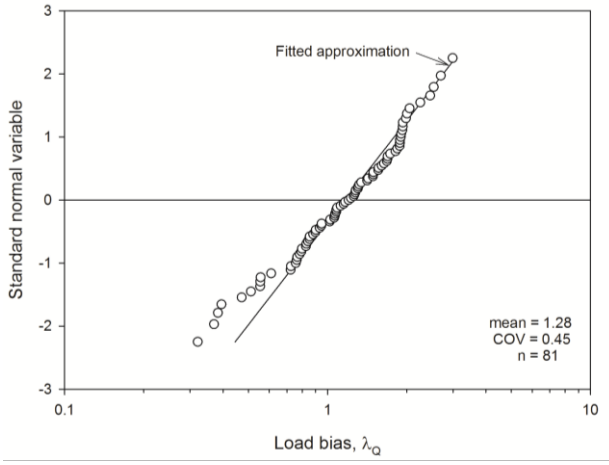

a) cumulative distribution function (CDF) plot

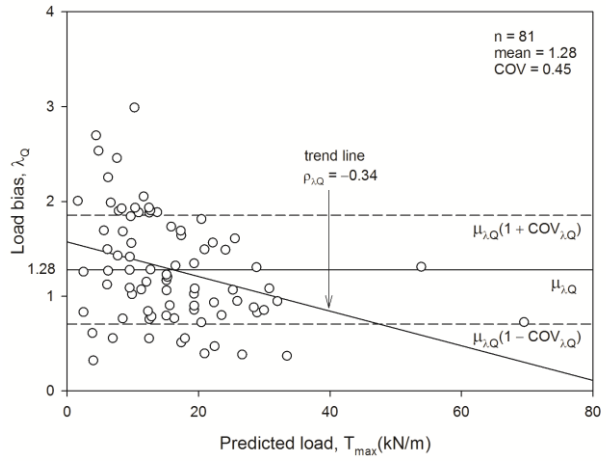

b) load bias versus predicted (nominal) load

Figure 3. Load bias statistics for using Coherent Gravity Method.

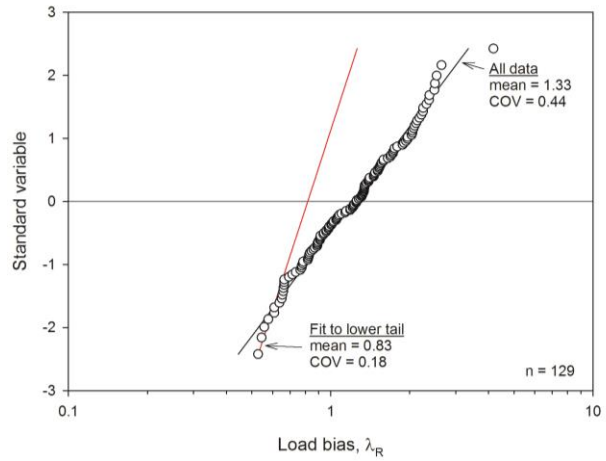

a) cumulative distribution function (CDF) plot

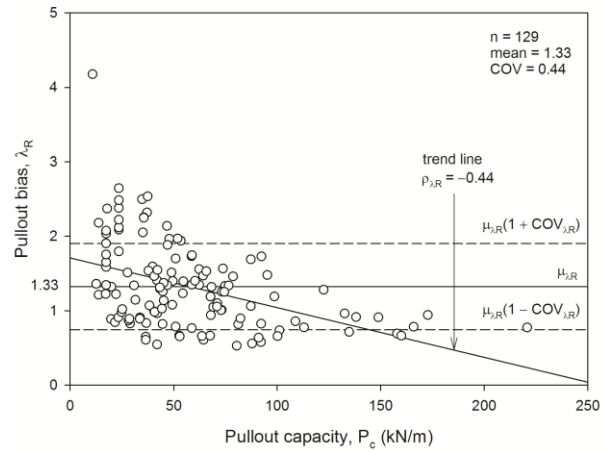

b) pullout bias versus predicted (nominal) pullout capacity

Figure 4. Pullout bias statistics using (AASHTO 2017) pullout model.

are correlated. This can be understood by inspecting the contents of Equation 2 and Equation 4. It can be seen that ϕ is present in the load model only, while γ appears in both load and pullout models. Lin and Bathurst (2018) showed that for limit state equations of the same general form as the pullout limit state in this paper, ρ_n can range from positive to negative depending on the magnitude of the COV values assumed for ϕ and γ. Inspection of Equation 5 shows that a positive nominal correlation value increases the value of β compared to $\rho_n = 0$ when all other conditions remain the same, and the reverse is true for $\rho_n < 0$. Ignoring the nominal correlation (i.e. setting $\rho_n = 0$) leads to a conservative estimate of β (error is on the safe side for design) when $\rho_n > 0$, and the opposite is true when the true value of ρ_n is negative. Assuming that the COV for the friction angle ϕ is $COV_\phi = 0.10$ and for the soil unit weight $COV_\gamma = 0.5$, the computed ρ_n for each layer using the method of Lin and Bathurst (2018) is in the vicinity of 0.3. Hence, setting $\rho_n = 0$ to simplify calculations results in a slightly conservative (i.e. safer design) outcome in the example wall calculations performed here. For a deeper treatment of this topic and guidance to calculate the nominal correlation, the reader is directed to the paper by Lin and Bathurst (2018).

In the following calculations the uncertainty in the calculation of nominal load and nominal pullout capacity (resistance) are assumed as equal for four different cases: $COV_{Qn} = COV_{Rn} = 0$, 0.1, 0.2 and 0.3. The plots show that for the top layer, probabilities of failure are greater than 1% for all levels of understanding. For the layer at z = 5.70 m, $P_f > 1\%$ only for $COV_{Qn} = COV_{Rn} = 0$. Again, as for the tensile strength limit state results, the probability of failure for each layer is largest when $COV_{Qn} = COV_{Rn} = 0$ and probabilities of failure for non-zero nominal COV cases do not change in the order expected intuitively.

The observation that the top layer is the most critical is not unexpected to experienced MSE wall designers. The remedy for any layer that does not satisfy the target P_f value of 1% is to do one or more of the following: 1) increase the number of transverse members (n_b) per element while maintaining the current reinforcement

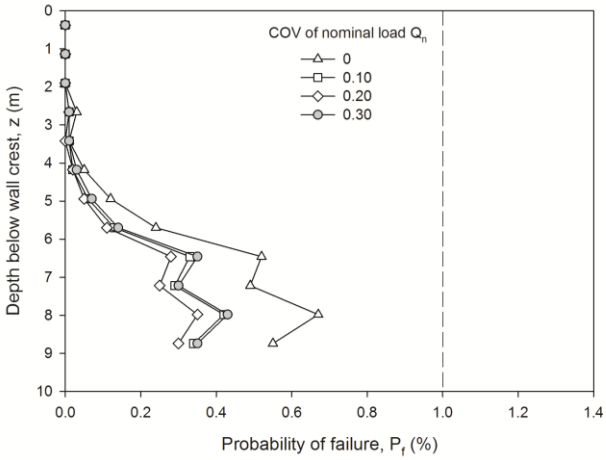

Figure 5. Probability of tensile strength failure for reinforcement layers in example wall assuming no corrosion.

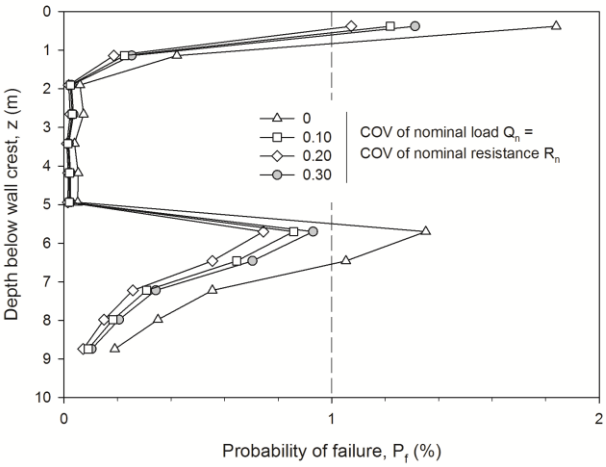

Figure 6. Probability of pullout failure for reinforcement layers in example wall assuming no corrosion.

length (L), 2) increase the length of the layer if the transverse bars are kept at the same spacing (this is the same result as 1); 3) increase the coverage ratio R_c of the streel grid reinforcement; 4) increase the transverse bar thickness. However, it is common practice to keep the transverse and longitudinal bar diameters the same.

8 CONCLUSIONS

The primary objective of this paper is to demonstrate the essential features of reliability-based design (RBD) for tensile strength and pullout limit states for MSE walls. To demonstrate the methodology, a steel grid reinforced soil wall has been used. However, the general approach applies to MSE walls reinforced with sheet geosynthetics (e.g. Bathurst et al. 2019), polymer straps and steel strips. There are differences in details related to the load and resistance models that appear in the limit state equations for these different systems, and each model will have different bias statistics.

In the particular example used in this paper, potential loss of tensile strength due to corrosion has not been considered in order to focus attention on the general RBD principles for this class of structure. However, loss of steel section due to consumption of the sacrificial zinc coating (galvanization) over the design life of steel reinforced MSE walls can be incorporated within the general framework described here as demonstrated by Allen et al. (2018) and Bozorgzadeh et al. (2019). However, if this is done, Monte Carlo simulation is required to compute probabilities of failure for both limit states.

REFERENCES

AASHTO. 2017. LRFD Bridge Design Specifications, 8th Ed., American Association of State Highway and Transportation Officials (AASHTO), Washington DC.

Allen, T.M. and Bathurst, R.J. 2018. Application of the Simplified Stiffness Method to design of reinforced soil walls. ASCE Journal of Geotechnical and Geoenvironmental Engineering 144(5): 04018024.

Allen, T.M., Bathurst, R.J. and Bozorgzadeh, N. 2019. Probabilistic tensile strength analysis of steel strips in MSE walls considering corrosion. ASCE Journal of Geotechnical and Geoenvironmental Engineering 145(5): 04019016-1-12.

Allen, T.M., Nowak, A.S. and Bathurst, R.J. 2005. Calibration to Determine Load and Resistance Factors for Geotechnical and Structural Design, Transportation Research Board Circular E-C079, Washington, DC, 93 p.

AASHTO. 2017. LRFD Bridge Design Specifications, 8th Ed., American Association of State Highway and Transportation Officials (AASHTO), Washington DC.

Allen, T.M. and Bathurst, R.J. 2018. Application of the Simplified Stiffness Method to design of reinforced soil walls. ASCE Journal of Geotechnical and Geoenvironmental Engineering 144(5): 04018024.

Allen, T.M., Nowak, A.S. and Bathurst, R.J. 2005. Calibration to Determine Load and Resistance Factors for Geotechnical and Structural Design, Transportation Research Board Circular E-C079, Washington, DC, 93 p.

Bathurst, R.J., Lin, P. and Allen, T.M. 2019. Reliability-based design of internal limit states for mechanically stabilized earth walls using geosynthetic reinforcement. Canadian Geotechnical Journal 56(6): 774-788.

Bathurst, R.J., Javankhoshdel, S. and Allen, T.M. 2017. LRFD calibration of simple soil-structure limit states considering method bias and design parameter variability. Journal of Geotechnical and Geoenvironmental Engineering 143(9): 04017053-1-14.

Bozorgzadeh, N., Bathurst, R.J. and Allen, T.M. 2019. Influence of corrosion on reliability-based design of steel grid MSE walls. Structural Safety (in review).

Canadian Highway Bridge Design Code. 2019. CAN/CSA-S6-14, Canadian Standards Association (CSA) Mississauga, Ontario, Canada.

Fenton, G.A., Naghibi, F., Dundas, D., Bathurst, R.J. and Griffiths, D.V. 2016. Reliability-based geotechnical design in the 2014 Canadian Highway Bridge Design Code. Canadian Geotechnical Journal 53(2): 236-251.

Lin, P. and Bathurst, R.J. 2018. Influence of cross-correlation between nominal load and resistance on reliability-based design for simple linear soil-structure limit states. Canadian Geotechnical Journal 55(2): 279-295.

Miyata, Y., Yu, Y. and Bathurst, R.J. 2018. Calibration of soil-steel grid pullout models using a statistical approach. ASCE Journal of Geotechnical and Geoenvironmental Engineering 144(2): 04017106.